

## High Conductivity in Hydrothermally Grown AgCuO<sub>2</sub> Single Crystals Verified Using Focused-Ion-Beam-Deposited Nanocontacts

David Muñoz-Rojas,<sup>\*,†,‡</sup> Rosa Córdoba,<sup>\*,§</sup> Amalio Fernández-Pacheco,<sup>\*,§,||</sup> José María De Teresa,<sup>§,||</sup> Guillaume Sauthier,<sup>‡</sup> Jordi Fraxedas,<sup>‡</sup> Richard I. Walton,<sup>#</sup> and Nieves Casañ-Pastor<sup>†</sup>

<sup>†</sup>Instituto de Ciencia de Materiales de Barcelona, ICMAB-CSIC, Campus de la UAB, Bellaterra 08193, Spain,

<sup>\*</sup>Instituto de Nanociencia de Aragón, <sup>§</sup>Departamento de Física de la Materia Condensada, Facultad de Ciencias, and

<sup>||</sup>Instituto de Ciencia de Materiales de Aragón, CSIC, Facultad de Ciencias, Universidad de Zaragoza, Zaragoza 50009,

Spain, <sup>‡</sup>Centro de Investigación en Nanociencia y Nanotecnología, CIN2 (CSIC-ICN), Campus de la UAB,

Bellaterra 08193, Spain, and <sup>#</sup>Department of Chemistry, University of Warwick, Coventry CV4 7AL, U.K.

Received July 16, 2010

The silver–copper mixed oxide AgCuO<sub>2</sub> (also formulated as Ag<sub>2</sub>Cu<sub>2</sub>O<sub>4</sub>) possesses a peculiar electronic structure in which both Ag and Cu are partially oxidized, with the charge being delocalized among the three elements in the oxide. Accordingly, a quasi-metallic behavior should be expected for this oxide, and indeed bulk transport measurements show conductivity values that are orders of magnitude higher than for other members of this novel oxide family. The presence of silver makes thermal sintering an inadequate method to evaluate true conductivity, and thus such measurements were performed on low density pellets, giving an underestimated value for the conductivity. In the present work we present a new synthetic route for AgCuO<sub>2</sub> based on mild hydrothermal reactions that has yielded unprecedented large AgCuO<sub>2</sub> single-crystals well over 1 μm in size using temperatures as low as 88 °C. We have used a dual beam instrument to apply nanocontacts to those crystals, allowing the in situ measurement of transport properties of AgCuO<sub>2</sub> single crystals. The results show a linear relationship between applied current and measured voltage. The conductivity values obtained are 50 to 300 times higher than those obtained for bulk low density AgCuO<sub>2</sub> pellets, thus confirming the high conductivity of this oxide and therefore supporting the delocalized charge observed by spectroscopic techniques.

### Introduction

1999 saw the birth of the new family of silver–copper mixed oxides, with Ag<sub>2</sub>Cu<sub>2</sub>O<sub>3</sub> being the first natural or synthetic silver–copper oxide ever known.<sup>1</sup> Research in this family was prompted by the need to find alternatives to the highest T<sub>c</sub> Hg–Cu based superconductors, in which the Hg could be replaced by a less hazardous element. Silver, presenting similarities in terms of chemistry and coordination with Hg, stands up as a good candidate to replace it. Although no superconductor phase has so far been discovered within the Ag–Cu oxide family, the new compounds found to date have shown very interesting structures and properties so as to deserve a deeper study in their own right. Thus, after the discovery of Ag<sub>2</sub>Cu<sub>2</sub>O<sub>3</sub>,<sup>1</sup> which was synthesized by a simple coprecipitation reaction,<sup>1</sup> other members were synthesized. Coprecipitation also yielded a solid solution of formula Ag<sub>3</sub>Pb<sub>2–x</sub>Cu<sub>x</sub>O<sub>6</sub>,<sup>2</sup> while oxidation of

Ag<sub>2</sub>Cu<sub>2</sub>O<sub>3</sub> performed chemically, that is, with ozone,<sup>3</sup> or electrochemically<sup>4,5</sup> yielded the third member in the family: Ag<sub>2</sub>Cu<sub>2</sub>O<sub>4</sub>. The same compound was also obtained from a AgNO<sub>3</sub> and Cu(NO<sub>3</sub>)<sub>2</sub> solution using persulfate as the oxidizing agent.<sup>6</sup> By a completely different approach, the azide/nitrate route gave rise to Rb<sub>3</sub>Ag<sub>0.5</sub>Cu<sub>0.5</sub>O<sub>2</sub>, a further member in the family, although air and moisture sensitive in this case.<sup>7</sup> Finally, a low-temperature hydrothermal reaction yielded the last family member so far described: AgCu<sub>0.5</sub>Mn<sub>0.5</sub>O<sub>2</sub>, a mixed B-site delafossite with significant magnetic properties.<sup>8</sup>

(3) Muñoz-Rojas, D.; Fraxedas, J.; Gómez-Romero, P.; Casañ-Pastor, N. *J. Solid State Chem.* **2005**, *178*, 295–305.

(4) Muñoz-Rojas, D.; Oró, J.; Gómez-Romero, P.; Fraxedas, J.; Casañ-Pastor, N. *Electrochem. Commun.* **2002**, *4*, 684–689.

(5) Muñoz-Rojas, D.; Tejada-Rosales, E. M.; Gómez-Romero, P.; Casañ-Pastor, N. *Bol. Soc. Esp. Ceram. Vidrio* **2002**, *41*, 55–58.

(6) (a) Curda, J.; Klein, W.; Jansen, M. *J. Solid State Chem.* **2001**, *162*, 220–224. (b) Curda, J.; Klein, W.; Liu, H.; Jansen, M. *J. Alloys Compd.* **2002**, *338*, 99–103.

(7) Sofin, M.; Peters, E.-M.; Jansen, M. *Z. Kristallogr. NCS* **2003**, *218*, 379–380.

(8) Muñoz-Rojas, D.; Subías, G.; Oró-Solé, J.; Fraxedas, J.; Martínez, B.; Casas-Cabanas, M.; Canales-Vázquez, J.; González-Calbet, J.; García-González, E.; Walton, R. I.; Casañ-Pastor, N. *J. Solid State Chem.* **2006**, *179*, 3883–3892.

\*To whom correspondence should be addressed. Present address: Department of Materials Science and Metallurgy, University of Cambridge, Pembroke Street, Cambridge CB2 3QZ, U.K. Phone: +441233334374. Fax: +441223334375. E-mail: davidmunozrojas@gmail.com.

(1) Gómez-Romero, P.; Tejada-Rosales, E. M.; Palacín, M. R. *Angew. Chem., Int. Ed.* **1999**, *38*, 524–525.

(2) Tejada-Rosales, E. M.; Oró-Solé, J.; Gómez-Romero, P. *J. Solid State Chem.* **2002**, *163*, 151–157.

Among these novel oxides,  $\text{AgCuO}_2$  presents very interesting crystallographic and electronic structures. This compound was initially reported as  $\text{Ag}_2\text{Cu}_2\text{O}_4$ , as it was obtained from the parent phase  $\text{Ag}_2\text{Cu}_2\text{O}_3$  (which implies an oxidation of +1 per unit formula of the latter). Although initial studies claimed, on the one hand, that copper was being oxidized from  $\text{Cu}^{2+}$  to  $\text{Cu}^{3+}$  basing it on structural studies under different conditions,<sup>6</sup> simultaneous X-ray photoelectron spectroscopy (XPS) analyses seemed to support a mixed valence for silver (i.e.,  $\text{Ag}^{1+x}\text{Ag}^{3+y}\text{Cu}^{2+z}\text{O}_4$ ).<sup>9</sup> Later, a deeper X-ray Absorption Spectroscopy (XAS) study showed that both metals are indeed partly oxidized and that the charge is actually delocalized among all the elements, including oxygen.<sup>10</sup> Thus, the XPS data was interpreted as an opening of the Ag 4d band, and a more detailed study of the O 1s signal showed also a true oxidation of oxygen atoms.<sup>9,10</sup> Therefore, the best way to describe this oxide is as  $\text{Ag}^{(1+x)}\text{Cu}^{(2+y)}\text{O}^{-(2-z)}$ , where the values of  $x$  and  $y$  depend on the synthetic method used, and in which all elements share an intermediate oxidation state.<sup>10</sup> More recent XAS studies performed by other groups using highly crystalline  $\text{AgCuO}_2$  samples have confirmed the charge delocalization and the oxidation of silver in the compound.<sup>11</sup>

On the crystallographic side,  $\text{AgCuO}_2$  is isostructural with crednerite ( $\text{CuMnO}_2$ ), having the space group  $C2/m$ .<sup>4</sup> But while copper atoms are linearly coordinated by 2 oxygen atoms in crednerite ( $\text{O}-\text{Cu}^{1+}-\text{O}$ ), the oxidized  $\text{Ag}^{(1+x)+}$  atoms in  $\text{AgCuO}_2$  are coordinated by 6 oxygen atoms, 2 axial and four equatorial forming an elongated octahedron, as deduced from extended X-ray absorption fine structure (EXAFS),<sup>10</sup> and accordingly to the higher oxidation state of silver (see Figure 1).

The peculiar electronic structure described above implies that  $\text{AgCuO}_2$  should be a quasi-metal in which the delocalized electrons would play the equivalent role of a partly filled conduction band.<sup>10</sup> A first hint on this high conductivity comes from contrasting the darker color of  $\text{AgCuO}_2$ , as compared with  $\text{Ag}_2\text{Cu}_2\text{O}_3$  or  $\text{AgCu}_{0.5}\text{Mn}_{0.5}\text{O}_2$ , in which the metals have a fixed oxidation state and no charge delocalization takes place. A second hint of the absence of localized  $\text{Ag}^{1+}$ ,  $\text{Cu}^{3+}$  states, is the absence of diamagnetism expected for those states, and the observation of a small Pauli paramagnetism typical of many metals,<sup>12</sup> checked for all pure samples in several measurement holders. The actual evaluation of the transport properties in these phases is not simple since the presence of silver does not allow any sintering and thus, dense pellets are difficult to obtain. In spite of such difficulties, bulk transport measurements have been reported for  $\text{Ag}_2\text{Cu}_2\text{O}_3$ ,<sup>13</sup>  $\text{AgCu}_{0.5}\text{Mn}_{0.5}\text{O}_2$ , and  $\text{AgCuO}_2$ ,<sup>12,14</sup> the latter presenting conductivity values orders of magnitude higher than the former two, as expected from their respective electronic structures, and thereby showing the predicted enhanced conductivity of  $\text{AgCuO}_2$  as a result of charge delocalization.

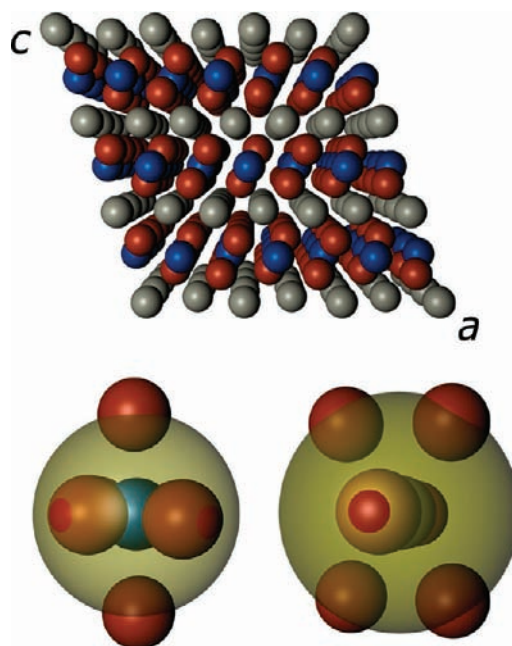


**Figure 1.** Crystallographic structure of  $\text{AgCuO}_2$ ; red, oxygen; blue, copper; gray, silver. All atoms are drawn with the same radius for the sake of clarity. While structurally equivalent to crednerite ( $\text{CuMnO}_2$ ), the coordination of the metals in  $\text{AgCuO}_2$  and, therefore, the electronic structure and oxidation states are completely different. As shown at the bottom, Ag is coordinated by six oxygen atoms forming a deformed octahedron (right). This octahedron is nevertheless more close to being regular than the one formed by the six closest oxygen atoms around Cu cations (left), as illustrated by the superimposed spheres; and indeed copper has a 4 planar square coordination only. The small distance of the 4 equatorial oxygen atoms around Ag (as compared for instance with  $\text{Ag}^{3+}$  coordination in  $\text{AgO}$ )<sup>10</sup> is what accounts for the higher oxidation state observed by spectroscopic techniques.

In addition to these results concerning bulk measurements, direct measurements on single crystals would be of most interest to better characterize the transport properties of  $\text{AgCuO}_2$ , by eliminating any contribution from grain boundaries. The presence of silver in this compound makes it very difficult to grow a single macroscopic crystal to allow a standard electrical measurement. However, nanotechnology tools can be brought into action to carry out electrical measurements at the micro/nanoscale. In this sense, Focused-Ion-Beam (FIB) or Focused-Electron-Beam (FEB) nanolithography can be used to pattern metallic nanocontacts by introducing metal-organic precursors in the process chamber, which become dissociated by the ion or electron beam,<sup>15</sup> the resolution of this process reaching down to a few nanometers. These techniques have been applied to the transport characterization of individual nanowires<sup>16</sup> and nanoparticles.<sup>17</sup> In addition, the use of in situ transport measurements inside a dual beam (FIB/FEB) is very useful to quickly characterize the conductive properties of nanostructures.<sup>18</sup>

(9) Muñoz-Rojas, D.; Oró, J.; Fraxedas, J.; Gómez-Romero, P.; Casañ-Pastor, N. *Cryst. Eng.* **2002**, *5*, 459–467.

(10) Muñoz-Rojas, D.; Subías, G.; Fraxedas, J.; Gómez-Romero, P.; Casañ-Pastor, N. *J. Phys. Chem. B* **2005**, *109*, 6193–6203.

(11) Dr. G. Waterhouse. Private Communication.

(12) Muñoz-Rojas, D. New Ag-Cu Oxides by Electrochemical Intercalation and other soft methods. Ph.D. Thesis, Autonomous University of Barcelona (UAB), Barcelona, Spain, May 2004.

(13) Tejada-Rosales, E. M.; Rodríguez-Carvajal, J.; Casañ-Pastor, N.; Alemany, P.; Ruiz, E.; El-Fallah, M. S.; Álvarez, S.; Gómez-Romero, P. *Inorg. Chem.* **2002**, *41*, 6604–6613.

(14) Sauvage, F.; Muñoz-Rojas, D.; Poeppelmeier, K. R.; Casañ-Pastor, N. *J. Solid State Chem.* **2009**, *182*, 374–380.

(15) Utker, I.; Hoffmann, P.; Melngailis, J. *J. Vac. Sci. Technol. B* **2008**, *26*, 1197–1276.

(16) Cronin, S. B.; Lin, Y. M.; Rabin, O.; Black, M. R.; Ying, J. Y.; Dresselhaus, M. S.; Gai, P. L.; Minet, J. P.; Issi, J. P. *Nanotechnology* **2002**, *13*, 653.

(17) Martínez-Boubeta, C.; Balcells, L.; Monty, C.; Ordejon, P.; Martínez, B. *Appl. Phys. Lett.* **2009**, *94*, 062507.

(18) (a) De Teresa, J. M.; Córdoba, R.; Fernández-Pacheco, A.; Montero, O.; Strichovanec, P.; Ibarra, M. R. *J. Nanomaterials* **2009**, 936863. (b) Fernández-Pacheco, A.; De Teresa, J. M.; Córdoba, R.; Ibarra, M. R. *Phys. Rev. B* **2009**, *79*, 174204.

**Table 1.** Summary of Different Reactions Assayed for the Hydrothermal Synthesis of AgCuO<sub>2</sub>

reaction no.	reactants/g	H <sub>2</sub> O/mL	T/°C	t	oxidizer/g	products
1	0.2 AgO, 0.2 CuSO <sub>4</sub> ·5H <sub>2</sub> O, 0.1 NaOH	12	240	10 h		Ag <sub>2</sub> O, CuO
2	0.2 AgO, 0.2 CuSO <sub>4</sub> ·5H <sub>2</sub> O, 0.1 NaOH	12	160	10 h		Ag <sub>2</sub> O, CuO, (AgCuO <sub>2</sub> )
3	0.13 AgO, 0.26 CuSO <sub>4</sub> ·5H <sub>2</sub> O, 0.3 KOH	12	120	10 h		AgCuO <sub>2</sub> , Ag <sub>2</sub> O
4	0.13 AgO, 0.26 CuSO <sub>4</sub> ·5H <sub>2</sub> O, 0.3 KOH	12	r.t.	17 h		AgCuO <sub>2</sub>
5	0.13 AgO, 0.18 CuSO <sub>4</sub> , 1 KOH	12	120	17 h	0.3 K <sub>2</sub> S <sub>2</sub> O <sub>8</sub>	AgCuO <sub>2</sub>
6	0.2 AgNO <sub>3</sub> , 0.28 Cu(NO <sub>3</sub> ) <sub>2</sub> ·3H <sub>2</sub> O, 2 KOH	36	100	17 h	1 K <sub>2</sub> S <sub>2</sub> O <sub>8</sub>	AgCuO <sub>2</sub> , Ag <sub>2</sub> O, CuO
7	0.4 Ag <sub>2</sub> Cu <sub>2</sub> O <sub>3</sub> , 6 KOH	36	90	20 h	2 K <sub>2</sub> S <sub>2</sub> O <sub>8</sub>	AgCuO <sub>2</sub>
8	0.13 AgO, 0.18 CuSO <sub>4</sub> , 8 KOH	30	88	17 d	1.5 K <sub>2</sub> S <sub>2</sub> O <sub>8</sub>	AgCuO <sub>2</sub> , Ag <sub>2</sub> O, CuO
9	0.1 Ag <sub>2</sub> Cu <sub>2</sub> O <sub>3</sub> , 4 KOH	36	88	15.5 d	2 K <sub>2</sub> S <sub>2</sub> O <sub>8</sub>	AgCuO <sub>2</sub> , (CuO)

The largest particles of AgCuO<sub>2</sub>, the ones obtained by electrochemical oxidation of Ag<sub>2</sub>Cu<sub>2</sub>O<sub>3</sub>, reach a maximum of only ~500 nm width, and several nanometers thickness.<sup>4</sup> Despite the fine resolution of the current dual-beam technology, these dimensions are still quite prohibitive and no reliable results could be obtained. To overcome this limitation we have developed a new synthetic route for AgCuO<sub>2</sub> based in low temperature hydrothermal reactions that have allowed us to synthesize crystals several micrometers in size for the first time. Hydrothermal reactions have proven very effective in the synthesis of complex oxides at relatively low temperatures in the past.<sup>19</sup> In this work we describe the hydrothermal synthesis of micrometric AgCuO<sub>2</sub> single crystals and the study of their transport properties by means of a Dual-Beam microscope.

## Experimental Section

**Materials and Characterization.** Reagent grade AgO (Aldrich), AgNO<sub>3</sub> (Panreac), CuSO<sub>4</sub> (PROBUS), CuSO<sub>4</sub>·5H<sub>2</sub>O (Fluka), Cu(NO<sub>3</sub>)<sub>2</sub>·3H<sub>2</sub>O (Merk), Sodium Persulfate (Na<sub>2</sub>S<sub>2</sub>O<sub>8</sub>, Aldrich), KOH, and NaOH were purchased and used as received. Ag<sub>2</sub>Cu<sub>2</sub>O<sub>3</sub> was synthesized as previously reported.<sup>1</sup>

The hydrothermal synthesis of AgCuO<sub>2</sub>, was performed in either a 23 mL Parr acid digestion bomb or a screw capped 60 mL plastic bottle. The different conditions and precursors tried are summarized in Table 1.

X-ray powder diffraction data were collected using a Rigaku X-ray powder diffractometer RotaflexRu-200B, with Cu Kα radiation. Scanning electron microscopy (SEM) was performed with a Hitachi S-570. XPS measurements were performed at room temperature with a SPECS EA10P hemispherical analyzer using non-monochromatic Mg Kα radiation (1253.6 eV) as excitation source in a base pressure of about 10<sup>-9</sup> mbar, on pressed pellets, avoiding using silver epoxy.

**In Situ Measurements of the Transport Properties.** For the present experiments, a commercial “dual beam” instrument (Nova 200 NanoLab from FEI) was used. It integrates a 30 kV field-emission electron column and a Ga-based 30 kV ion column placed forming 52° with coincidence point 5 mm away from the electron-column pole. The contacts on the microparticles were performed by means of Pt or W deposition using an automatized gas-injection system (GIS), with (CH<sub>3</sub>)<sub>3</sub>Pt(CpCH<sub>3</sub>) (trimethylcyclopentadienyl-platinum) and W(CO)<sub>6</sub> (tungsten hexacarbonyl) as the precursors, respectively. The GIS tip was positioned about 150 μm away from the region of interest in the z direction and about 50 μm away in the x/y direction. The GIS was heated to about 40 °C for operation and a 10-min preheating period was performed before deposition. In the case of Pt, contacts made with focused-ion-beam-induced deposition results in low contact resistance compared to focused-electron-beam-induced deposition and were thus preferred for the present study.<sup>18a</sup> W contacts were also deposited by FIB. To perform the

electrical measurements, a drop of the microparticle-containing suspension is first deposited onto a thermally oxidized silicon wafer (~200 nm of SiO<sub>2</sub> on top of the Si substrate) where Al microelectrodes have been pre-patterned in a well-defined geometry to enable transport measurements by means of conventional optical lithography. The final mask consist of large metallic pads (400 μm × 400 μm), which are connected via 4 μm wide electrodes. The target microparticle was located by means of the electron microscope, and Pt or W nanocontacts were patterned on the microparticle, connecting it to the Al-microelectrodes. The experimental setup to measure in situ the resistance by four-point method without breaking vacuum has been previously used in our group in Pt-based nanodeposits<sup>18</sup> and Co-based nanodeposits.

## Results and Discussion

**Hydrothermal Synthesis of AgCuO<sub>2</sub>.** The hydrothermal synthesis of AgCuO<sub>2</sub>, was performed from starting products matching the formal oxidation state in the final product, as it would be the case in an ordinary high temperature solid state reaction. Following such approach, solid AgO (in which half of the silver atoms have oxidation state of +3, according to the formula Ag<sup>+</sup>Ag<sup>3+</sup>O<sub>2</sub>)<sup>20</sup> was suspended in an Cu(SO<sub>4</sub>)<sub>2</sub> solution, according to a 1:1 metal molar ratio. NaOH or KOH was then added to act as mineralizer, and the suspension was stirred for 5 min before the hydrothermal treatment at different temperatures. (Hydrothermal heterogeneous redox reactions, that is, using a solid insoluble reactant instead of a soluble salt, have proven a very effective path to the formation of novel oxide phases<sup>8</sup> and even remarkable hybrid nanostructures<sup>21</sup>.) Table 1 shows a summary of different reactions performed and the respective products obtained. The corresponding X-ray diffraction (XRD) patterns are presented in Figure 2.

As shown in Table 1, the product of the reaction is very sensitive to the temperature used and, thus, only Ag<sub>2</sub>O and CuO were obtained when the reaction was carried at 240 °C (reaction 1). On the contrary, when the temperature was lowered to 160 °C some tiny peaks corresponding to AgCuO<sub>2</sub> could be observed along with those of Ag<sub>2</sub>O and CuO (reaction 2, see small black arrows in Figure 2). In reactions 1 and 2 in Table 1, an excess of AgO was used so that the possible formation of AgCuO<sub>2</sub> could be achieved in spite of the expected high reduction rate of AgO to give Ag<sub>2</sub>O. At 120 °C the main product was already AgCuO<sub>2</sub>, but the presence of other products, especially Ag<sub>2</sub>O (as in reaction 3 for instance), was very hard to avoid. Finally, and very interestingly, an equivalent reaction carried out at room

(20) Fischer, P.; Jansen, M. *J. Less-Common Met.* **1988**, *137*, 123–131.

(19) (a) Sheets, W. C.; Mugnier, E.; Barnabe, A.; Marks, T. J.; Poepplmeier, K. R. *Chem. Mater.* **2006**, *18*, 7–20. (b) Sheets, W. C.; Stampfer, E. S.; Bertoni, M. I.; Sasaki, M.; Marks, T. J.; Mason, T. O.; Poepplmeier, K. R. *Inorg. Chem.* **2008**, *47*, 2696–2705. (c) Modeshia D. R.; Walton, R. I. *Chem. Soc. Rev.* **2010**, *39*, 4303–4325.

(21) (a) Muñoz-Rojas, D.; Oró-Solé, J.; Ayyad, O.; Gómez-Romero, P. *Small* **2008**, *4*, 1301–1306. (b) Muñoz-Rojas, D.; Oró-Solé, J.; Gómez-Romero, P. *J. Phys. Chem. C* **2008**, *112*, 20312–20318. (c) Muñoz-Rojas, D.; Oró-Solé, J.; Gómez-Romero, P. *Chem. Commun.* **2009**, 5913–5915. (d) Muñoz-Rojas, D.; Oró-Solé, J.; Ayyad, O.; Gómez-Romero, P. *J. Mater. Chem.* DOI:10.1039/C0JM01449D.

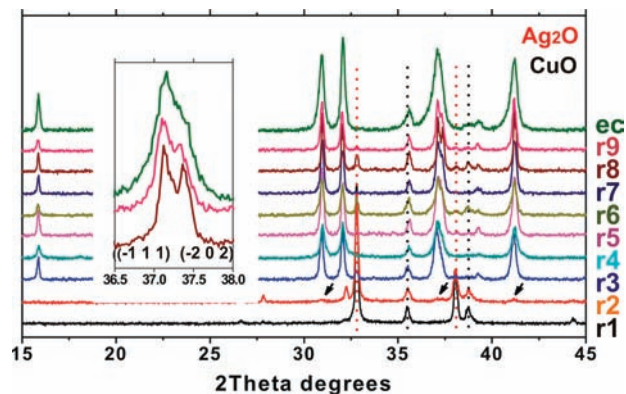


**Figure 2.** XRD patterns of the products obtained for the different hydrothermal reactions summarized in Table 1. The red and black dotted lines point to the main  $\text{Ag}_2\text{O}$  and  $\text{CuO}$  peaks that can be observed in some of the samples.

temperature for 17 h (see Table 1) yielded  $\text{AgCuO}_2$  as the sole product. Solid  $\text{AgO}$  is therefore capable of oxidizing the  $\text{Cu}^{2+}$  ions in the suspension to form the mixed oxide even at room temperature and ambient pressure. Under hydrothermal conditions the mechanism is equivalent to other methods, with  $\text{AgO}$  being the oxidizing agent to finally form  $\text{AgCuO}_2$  which contains both oxidized silver and copper.<sup>3</sup> The mixed oxide is less stable as temperature increases and tends to decompose to  $\text{Ag}_2\text{O}$  and  $\text{CuO}$  and/or other copper species in solution (soluble complexes formed at high pH) in those conditions. Higher temperatures also accelerate the reduction of  $\text{AgO}$  to  $\text{Ag}_2\text{O}$  before  $\text{AgCuO}_2$  can even be formed, which would explain the absence of  $\text{AgCuO}_2$  in reaction 1 (at 240 °C) and the low yield in reaction 2 (at 160 °C). On the contrary, it is interesting to note that metallic silver is never obtained, not even at 240 °C, the reduction of  $\text{AgO}$  proceeding to form  $\text{AgCuO}_2$  (in which the silver ions have an oxidation state of  $1 + x$ ) or  $\text{Ag}_2\text{O}$  for the higher temperatures. This is quite different to what happens at ambient pressure, conditions in which silver is readily reduced to metallic Ag as the temperature is increased (around 100 °C for  $\text{AgO}$  and 200 °C for  $\text{Ag}_2\text{O}$ ).<sup>22</sup>

Figure 3 shows SEM images for different  $\text{AgCuO}_2$  samples. In Figure 3a, crystals obtained by electrochemical oxidation of  $\text{Ag}_2\text{Cu}_2\text{O}_3$  can be observed. Figure 3b shows some of the crystals obtained in reaction 3 (Table 1), in which  $\text{AgCuO}_2$  was the main product. Although the sample presents a high dispersion in particle size, particles of up to about 3  $\mu\text{m}$  could be found, as opposed to what is observed for electrochemically synthesized  $\text{AgCuO}_2$ , which presents much smaller particles.

In an effort to minimize the formation of  $\text{Ag}_2\text{O}$  and  $\text{CuO}$  at 120 °C and higher temperatures, and favor the formation of pure  $\text{AgCuO}_2$  with even higher particle sizes, an additional oxidizing agent, namely, sodium persulfate,  $\text{Na}_2\text{S}_2\text{O}_8$ , was added to the initial suspension. Under these conditions, the formation of  $\text{AgCuO}_2$  could be achieved at 120 °C without any  $\text{Ag}_2\text{O}/\text{CuO}$  impurities being obtained (reaction 5). Notwithstanding, even when using persulfate, great care had to be taken to avoid the formation of byproduct. From the output of many other reactions carried out (not shown) we could conclude that higher pHs, higher amounts of persulfate,

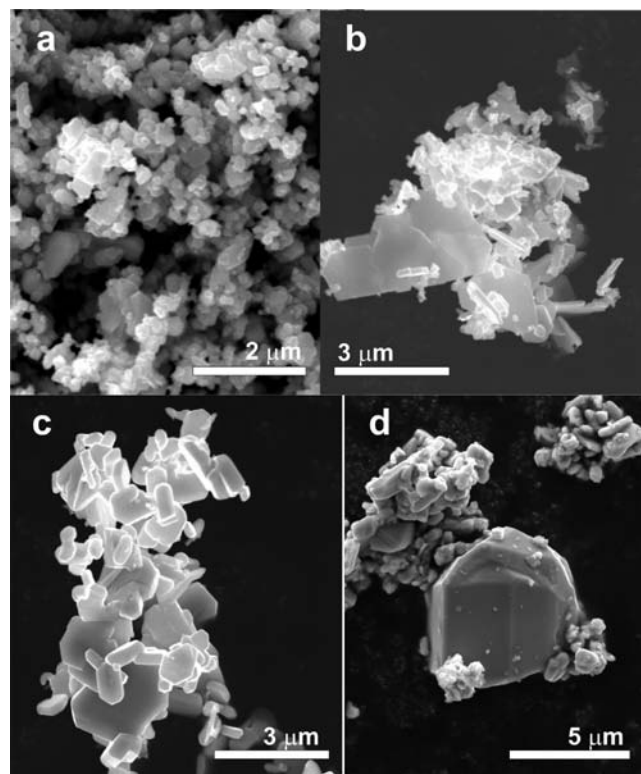


**Figure 3.** SEM images of (a)  $\text{AgCuO}_2$  obtained by electrochemical oxidation of  $\text{Ag}_2\text{Cu}_2\text{O}_3$ ; and via mild hydrothermal reactions: (b) product obtained using  $\text{AgO}$  and  $\text{CuSO}_4$  as starting products (reaction 3 in Table 1); (c) product obtained using  $\text{Ag}_2\text{Cu}_2\text{O}_3$  and persulfate as starting products (reaction 7 in Table 1); (d) product obtained using  $\text{AgO}$  and  $\text{CuSO}_4$  and a temperature of 88 °C during 17 days (reaction 8 in Table 1).

and a better mixing before the hydrothermal treatment translated to higher yields. Having persulfate as oxidizing agent also allowed the use of soluble  $\text{AgNO}_3$  as silver source (similarly to the method reported in ref 6), instead of solid  $\text{AgO}$ , though in this case  $\text{CuO}$  and  $\text{Ag}_2\text{O}$  were hard to avoid (see reaction 6 for instance). In a slightly different approach, and to avoid diffusion (kinetic) limitations that could be facilitating the precipitation of  $\text{Ag}_2\text{O}$  or  $\text{CuO}$  before the mixed oxide could form, a suspension of  $\text{Ag}_2\text{Cu}_2\text{O}_3$  was used, as opposed to using different precursors for Ag and Cu (see reaction 7 in Table 1). This again yielded pure  $\text{AgCuO}_2$ , but even though the formation of  $\text{Ag}_2\text{O}$  or  $\text{CuO}$  was easier to avoid at temperatures below 100 °C in this case, the increase in temperature translated to more byproduct being obtained. Figure 3c shows an image of the particles obtained for reaction 7 in Table 1 (using  $\text{Ag}_2\text{Cu}_2\text{O}_3$  and persulfate) where crystals over 2  $\mu\text{m}$  in size can be observed despite using a temperature of only 90 °C for the synthesis.

As it was stated in the introduction,  $\text{AgCuO}_2$  presents a delocalized charge distribution with silver and copper having oxidation states of  $1 + x$  and  $2 + y$ , respectively.<sup>10</sup> The values of  $x$  and  $y$  are different for different synthetic methods and can also vary under strong radiation.<sup>9</sup> Because of this particular electronic configuration,  $\text{AgCuO}_2$  could be considered a quasi-metal, and indeed bulk conductivity measured in pressed pellets is several orders of magnitude larger than that of  $\text{AgCu}_{0.5}\text{Mn}_{0.5}\text{O}_2$ <sup>14</sup> or  $\text{Ag}_2\text{Cu}_2\text{O}_3$ .<sup>13</sup> To probe the valence of silver cations in the samples obtained using the new hydrothermal approach, XPS was performed. XPS has proven a very sensitive and effective tool to probe

(22) *CRC Handbook of Chemistry and Physics*, 85th ed.; CRC Press: Boca Raton, FL, 2004.

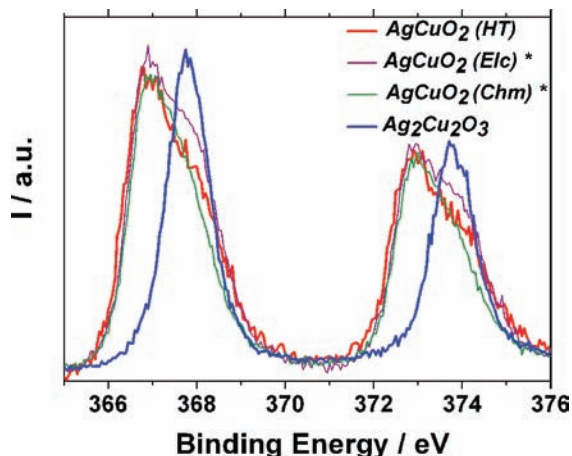


**Figure 4.** 3d region of the XPS spectra of  $\text{Ag}_2\text{Cu}_2\text{O}_3$  and  $\text{AgCuO}_2$  synthesized under hydrothermal conditions (reaction 9 in Table 1). \* The XPS spectra of electrochemically and chemically synthesized  $\text{AgCuO}_2$  samples (from reference 10) are also included for comparison.

the electronic state of Ag in  $\text{AgCuO}_2$ , showing a clear shift to lower binding energies of the Ag 3d band, as compared to that of  $\text{Ag}_2\text{Cu}_2\text{O}_3$  or  $\text{Ag}_2\text{O}$ . In some cases the spectrum presents two clearly separate peaks. Figure 4 shows the XPS spectra of the Ag 3d region for  $\text{Ag}_2\text{Cu}_2\text{O}_3$  and for the  $\text{AgCuO}_2$ , obtained in reaction 7. XPS spectra of  $\text{AgCuO}_2$  prepared by electrochemical and chemical oxidation are also included for comparison (the spectra are taken from reference 10). A clear shift of both the Ag 3d<sub>3/2</sub> and Ag 3d<sub>5/2</sub> bands to lower energies for  $\text{AgCuO}_2$ , as compared with  $\text{Ag}_2\text{Cu}_2\text{O}_3$ , is clearly observed being equivalent to that observed for  $\text{AgCuO}_2$  samples prepared by other methods,<sup>10</sup> as shown in Figure 4; this represents unequivocal evidence that silver has an oxidation state higher than 1+ in hydrothermally synthesized  $\text{AgCuO}_2$ , as was indeed expected. The XPS spectrum for the O 1s region is also similar to the one obtained for other  $\text{AgCuO}_2$  samples (not shown).<sup>10</sup> Thus, it can be concluded that the product obtained using the hydrothermal approach has a similar electronic structure to those obtained by other means, and thereby, high conductivity values should be expected. On the other hand, the influence of the synthetic method in the electronic structure can still be observed in the different shape of the XPS spectrum for the hydrothermal  $\text{AgCuO}_2$ , as compared to the ones obtained for  $\text{AgCuO}_2$  synthesized by other methods.<sup>10</sup>

**Transport Properties of  $\text{AgCuO}_2$  Single Crystals.** For the in situ transport measurements, the reaction conditions were adjusted to favor the formation of big particles. In particular, mild hydrothermal reactions at 88 °C were carried during long periods, namely, 15.5 days using  $\text{Ag}_2\text{Cu}_2\text{O}_3$  and persulphate (reaction 8 in Table 1). The XRD pattern of this sample clearly indicates a significant increase in average particle size, as deduced from the much better resolved peaks, as compared with the electrochemical sample (see inset in Figure 1). SEM confirmed the larger average particle size, which is caused by the long reaction times used in this case. Figure 3d shows a single crystal of over 5  $\mu\text{m}$  in size obtained for reaction 8, along with smaller particles. The mild temperature used favored the minimal decomposition of  $\text{AgCuO}_2$ , and only small amounts of CuO were present after such long reaction times (see XRD pattern in Figure 2).

As explained in the Experimental Section, the sample was then scanned to find big isolated particles to be contacted. Figure 5 shows an example of a particle of  $\text{AgCuO}_2$  from reaction 9 contacted using Pt as described in the Experimental Section. The particle has approximate dimensions of  $1 \times 1 \times 3 \mu\text{m}$ , and does not show any observable damage caused by the ion beam used to make the contacts. The particle seems to be the result of twinning (as is the case for many of the big particles obtained using the hydrothermal method, shown in Figure 3), yet it can be considered a single crystal since both twin crystals are clearly welded and aligned at the bottom face (see insets in Figure 5). The EDX also shows that the particle contains both Ag and Cu (1:1 ratio), thus confirming that it is a crystal of  $\text{AgCuO}_2$  and not a  $\text{Ag}_2\text{O}$  or CuO impurity.

Contacting the particles was indeed highly challenging because of their height (1  $\mu$  or over) and their low aspect ratio. Most in situ transport measurements reported to date have been performed by applying nanocontacts to nanowires or nanotubes, which have a maximum diameter of some tens of a nanometer. One-dimensional (1D) nanostructures are easily contacted by laying the nanocontact over the wire/tube and without risk of shortcircuit between the different contacts because of their high aspect ratio. In this work, we have successfully applied neat nanocontacts on 1  $\mu\text{m}$  tall particles with an aspect ratio as low as 3:1.

Once the particle was contacted, in situ four-probe current versus voltage measurements were performed. To check the quality of the contacts, initial 2-probe measurements were made, using alternative couples of nanocontacts. In both cases, a linear dependence between applied current and voltage was obtained. Linear fitting of the lines obtained for the different set of nanocontacts gave comparable resistance values of 250.6 and 235.0 k $\Omega$ , respectively, thus indicating the good quality of the nanocontacts on the  $\text{AgCuO}_2$  particle. 4-Probe in situ measurements were then made using the four nanocontacts simultaneously. To avoid any risk of short-circuit between the nanocontacts, the two intensity probes were connected to nanocontacts placed in opposite corners of the crystal. The measurements again showed a linear dependence between applied current and voltage, as shown in Figure 6, which corresponds to the contacted particle shown in Figure 5. Linear fitting of the obtained points gave a resistance value of 1.75 k $\Omega$ . This value is much smaller than the one obtained for 2-probe measurements, and consistent with the high conductivity expected for  $\text{AgCuO}_2$ . Taking into account the particle shape, and the resistance obtained from the four-probe measurement, we calculated a conductivity value of  $\sim 17 \text{ S cm}^{-1}$  for  $\text{AgCuO}_2$ . Similar results were obtained for another particle contacted with W instead of Pt (see Figure 6). In-situ four-probe current versus voltage measurements again showed a linear dependence when using W contacts. In this case, the resistance values obtained for 2-probe measurements were 51.0 and 49.2 k $\Omega$ , while the 4-probe measurement showed a resistance value of 0.2 k $\Omega$ . Taking into account the shape of the particle, the conductivity value obtained was in this case  $\sim 98 \text{ S cm}^{-1}$ . The difference in conductivity obtained for different nanocontacts can be due to either the difference in conductivity between the nanocontacts themselves or the error associated with the geometrical effects when measuring resistance in non-symmetric and small objects.<sup>23</sup> FIB-W

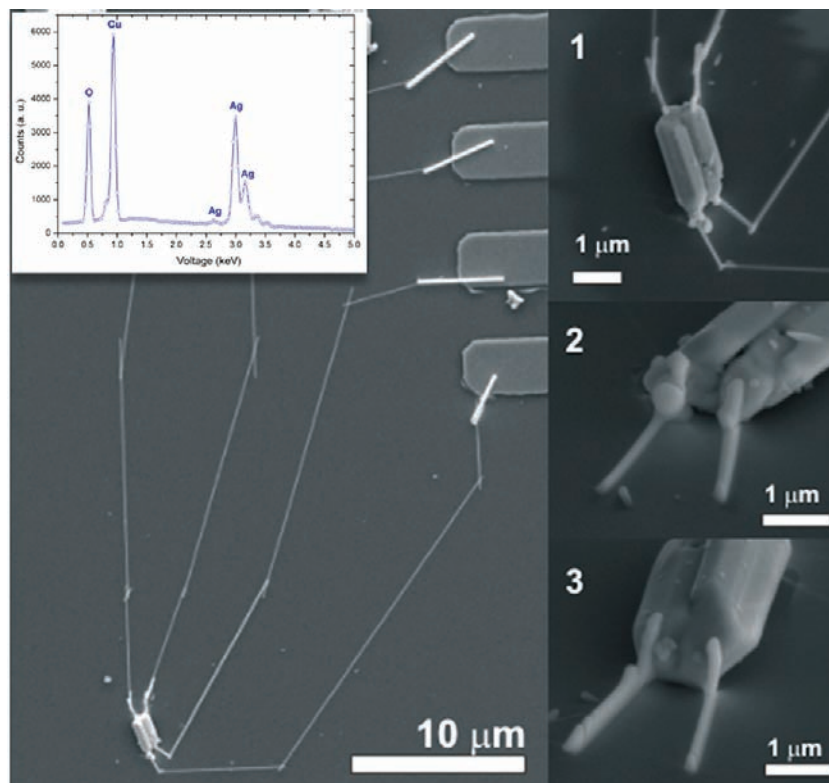


**Figure 5.** SEM image of a  $\text{AgCuO}_2$  particle from reaction 8 contacted using ion assisted deposition of Pt. The insets show a close-up of the particle from different perspectives, as well as an EDX spectrum of the contacted particle showing the corresponding peaks for Ag and Cu.

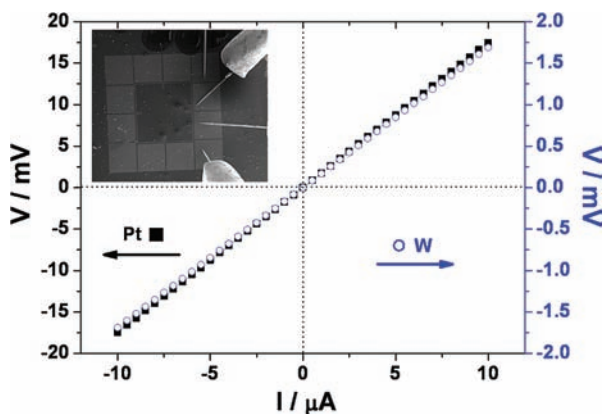


**Figure 6.**  $V$  versus  $I$  plots obtained for contacted particles using FIB-Pt and FIB-W nanocontacts. The inset shows the 4 probes contacting the patterned Al microelectrodes in the wafer, to which the metallic nanowires, Pt in this case, are connected. The nanocontacted  $\text{AgCuO}_2$  particle is in this case the one shown in Figure 5.

nanocontacts are indeed much more conducting than FIB-Pt ones,<sup>24</sup> as can be appreciated in the resistance values obtained for 2-probe measurements.

The conductivity values obtained in situ for  $\text{AgCuO}_2$  single crystals were thus 50 to 300 times higher than the one obtained for bulk measurements using nonsintered pellets.<sup>14</sup> Such a difference is not surprising given the fact that the bulk measurements were done with low-density, non-sintered pellets to avoid the formation of metallic

silver that occurs upon sintering. These measurements are then expected to be affected by an important component because of grain boundary resistance and, therefore, give only an underestimated value of the actual conductivity of  $\text{AgCuO}_2$ . The in situ measurements presented here thus confirm the high conductivity of  $\text{AgCuO}_2$ , and yield a closer estimation of the actual value. Although not a direct evidence, the results presented here are a necessary consequence of the charge delocalization among Ag, Cu and O observed using spectroscopic techniques (XPS, XANES, and EXAFS).<sup>10</sup>

## Conclusions

A new synthetic route for the synthesis of micrometer-sized  $\text{AgCuO}_2$  twinned and single crystals has been developed using mild hydrothermal reactions. Although the synthesis is possible using several precursors, the best results are obtained when  $\text{Ag}_2\text{Cu}_2\text{O}_3$  and persulfate are used at temperatures below 100 °C and for long reaction times. Using this novel approach, single crystals of several micrometers have been obtained for the first time, using temperatures as low as 88 °C. The big crystals obtained have been used to get a better estimation of the conductivity of  $\text{AgCuO}_2$ . In situ 4 probe measurements of nanocontacted  $\text{AgCuO}_2$  particles show a linear dependence between voltage and current, and the resistance values calculated are between 50 and 300 times smaller than those obtained for bulk measurements using low density pellets. Therefore, the present results confirm the high conductivity expected for  $\text{AgCuO}_2$  and, furthermore, they add to the consistency of the set of previously reported observations that evidence that the phase has an electronic structure similar to that found in the field of high  $T_c$  superconducting cuprates; and

(24) Marcano, N.; Sangiao, S.; Plaza, M.; Pérez, L.; Fernández Pacheco, A.; Córdoba, R.; Sánchez, M. C.; Morellón, L.; Ibarra, M. R.; De Teresa, J. M. *Appl. Phys. Lett.* **2010**, *96*, 082110.

that by itself constitutes an unique example from the more fundamental point of view in the field of argentates, cuprates, and mixed valence oxides.

**Acknowledgment.** The authors thank financing from Nanoaracat and from the Spanish Ministry of Education

and Science through Grants MAT2005-07683-C02-01 and MAT2008-06643-C02-01, and for a FPI fellowship for D.M-R. D.M-R. is also grateful to the CSIC and the European Social Fund for funding through the I3P program. Dr. F. Sauvage is acknowledged for fruitful discussions.